Gait-Cycle-Driven Transmission Power Control Scheme for a Wireless Body Area Network

Weilin Zang and Ye Li, *Member, IEEE*

***Abstract*—In a wireless body area network (WBAN), walking movements can result in rapid channel fluctuations, which severely degrade the performance of transmission power control (TPC) schemes. On the other hand, these channel fluctuations are often periodic and are time-synchronized with the user's gait cycle, since they are all driven from the walking movements. In this paper, we propose a novel gait-cycle-driven transmission power control (G-TPC) for a WBAN. The proposed G-TPC scheme reinforces the existing TPC scheme by exploiting the periodic channel fluctuation in the walking scenario. In the proposed scheme, the user's gait cycle information acquired by an accelerometer is used as beacons for arranging the transmissions at the time points with the ideal channel state. The specific transmission power is then determined by using received signal strength indication (RSSI). An experiment was conducted to evaluate the energy efficiency and reliability of the proposed G-TPC based on a CC2420 platform. The results reveal that compared to the original RSSI/link-quality-indication-based TPC, G-TPC reduces energy consumption by 25% on the sensor node and reduce the packet loss rate by 65%.**

***Index Terms*—Gait cycle, RSSI, transmission power control, wireless body area network (WBAN).**

I. Introduction

WIRELESS body area network (WBAN) is a promising technology that continuously collect the physiological (e.g., the heartbeat, blood pressure, electrocardiogram data, blood glucose, oxygen levels, and motion data) for ubiquitous healthcare services [1], [2]. A WBAN ordinarily consists of one sink node and several sensor nodes. The sink node, which is typically a mobile phone or another kind of portable device, collect sensory data from the sensor nodes and forwards the information to remote servers or a medical cloud platform [3] through a public network for further processing.

Energy efficiency in WBAN technology is a significant issue because most WBAN sensor nodes have limited battery capacity, yet in order to be used in healthcare monitoring they need to be able to for long period of time. Radio transmission is one of the most energy consuming operations for WBAN sensor nodes. Therefore, it is necessary to optimize the transmission power. Reliability is also necessary for medical services because the collected biological signals contain critical information that can have significant effects on patient health. Wireless on-body links are always dynamic because of body movement. For instance, a sensor mounted on a limb experiences a wide range of motion when the user is in mobility, which can result in a large fluctuation of link quality [4], [5]. In this case, in order to ensure the quality of the service, the transmission power must be high enough because the channel may temporarily experience high attenuation at certain time points. As a consequence, a static transmission power scheme can result in either poor energy efficiency or low reliability.

In order to overcome these issues, a number of transmission power control (TPC) protocols [6],[7] have been developed to improve energy efficiency and reliability in WBAN by adapting the transmission power to the link state in real time. TPC schemes in WBAN use RSSI samples associated with data packets that are sent by the transmitter to evaluate the current channel condition, and then accordingly adjust the output power of the transmission. An unreliable evaluation of the channel condition can result in failure of TPC. Therefore a rapid dynamic scenario, such as when the user is walking and the sensor nodes are deployed on the limbs, pose a great challenge for evaluating the channel condition because the acquired link state information is always outdated by the time of the next transmission. Unfortunately, rapid dynamic scenarios are the norm in WBAN since users are typically in mobility. One option for solving this problem is to send extra control packets. However, this approach introduces more control traffic leading to higher energy consumption on sensor nodes.

Continuous body movements present a challenge for TPC, but also result in periodic link quality fluctuation as body movements are always periodic during walking or running [4]. When data transmissions occur at the ideal point of the link quality the transmission power is reduced and reliability is guaranteed. In this paper we propose a novel TPC scheme that aims to exploit the periodic fluctuation of link quality by using the gait

Manuscript received August 28, 2016; revised December 31, 2016 and March 8, 2017; accepted March 19, 2017. Date of publication March 27, 2017; date of current version May 3, 2018. This work was supported in part by the National Natural Science Foundation of China under Grant 61379136, in part by Guangdong Province Special Support Program under grant 2014TX01X060, in part by the 863 Program under Grant SS2015AA02010, in part by Science and Technology Planning Project of Guangdong Province under Grant 2015B010129012, and in part by the Shenzhen Basic Research Funds under Grant JCYJ20160531184646437 and Grant JCYJ20140417113430655. *(Corresponding author: Ye Li.)*

The authors are with the Key Laboratory for Health Informatics of Chinese Academy of Sciences, Shenzhen Institutes of Advanced Technology, Chinese Academy of Sciences, Shenzhen, China. Shenzhen College of Advanced Technology, University of Chinese Academy of Sciences (e-mail: wl.zang@siat.ac.cn; ye.li@siat.ac.cn).

This paper has supplementary downloadable material available at http://ieeexplore.ieee.org.

Digital Object Identifier 10.1109/JBHI.2017.2688401

cycle as beacon to arrange the transmissions. The link quality fluctuation in many node deployments, such as wrist to chest or pants pocket to chest, is naturally time-synchronized with the gait cycle because they are driven from the same source (the walking movements). The proposed scheme first determines whether the user is walking or stationary (sitting or standing). If the user is walking, the proposed scheme acquires the user's gait cycle information by using the acceleration signal and learn the relationship between the gait cycle and the time points of the ideal channel condition. Then the transmissions are scheduled at time points when the link is temporarily in ideal state. The specific transmission power is determined by using received signal strength indication (RSSI). When the user is stationary, G-TPC operates as conventional TPC which is sufficient and cost-effective for the stationary scenario. To demonstrate the advantages of G-TPC, we conduct an experiment to evaluate the energy efficiency and reliability of G-TPC based on the CC2420 module. Six subjects were recruited to participate in the experiment and a total of 4 hours of data was collected. The experiment results reveal that compared to RSSI/LQI Based Transmission Power Control (RL-TPC) [8], energy consumption is reduced by 25% on the sensor node and packet loss rate is reduced by 65%.

The main contributions of the work are: 1) a novel gait cycle driven transmission power control scheme (G-TPC) which exploits the periodic fluctuation of link quality by using gait cycle information. Unlike conventional TPC schemes, G-TPC both adjusts the transmission power and also schedules transmissions at beneficial time points, which significantly improves TPC performance in walking scenario. The proposed scheme offers a new way of implementing TPC for use in WBAN; 2) validation of G-TPC through an experiment in which real world data is used. To address the challenge of the rapid channel fluctuation, we consider the node placement of ankle to pant pocket in the walking scenario in the experiment. To faithfully reflect the real daily life scenario, changes in activity (between walking and standing), and variants in walking speed are considered. We believe the experiment demonstrates the effectiveness and practicality of G-TPC.

In this study, we focus on the walking scenario. Individuals spend a small portion of their daily life walking, however, it remains one of the major challenges of TPC in WBAN (Stationary scenarios like sitting and standing are well managed in conventional TPC [6], [7]). Further, to reduce power consumption, the sensor node can go into standby mode when the user is not moving in applications like pedometer, energy expenditure estimation, pedestrian dead reckoning and real-time gait event detection. Therefore, improving the TPC scheme in the walking scenario can have significant benefits. The proposed scheme explores the relationship between the gait cycle and the time points of the ideal channel condition before communication; therefore, we do not assume any specific node placement. To acquire the user's gait cycle information, an accelerometer is required only at the sink node. There is no restriction on the physiology sensor at the sensor node.

The remainder of the paper is organized as follows. Section II provides an overview of related works. Section III introduces periodic channel fluctuation with experimental investigation. Section IV focuses on G-TPC scheme, including the system structure, user state detection, gait template extraction, transmission time location and transmission power determination. Section VI provides the experiment results and a performance comparison. Section V discusses the overhead of G-TPC with respect to buffer delay and computation load. The final section offers concluding remarks and suggestions for future work.

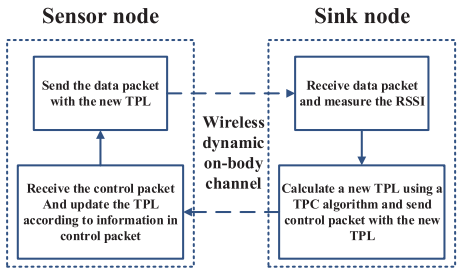

Fig. 1. Typical WBAN TPC system.

II. Related Work

The transmission power control (TPC) is a well-studied research area in WBAN, as it provides a simple and practical method for achieving energy efficiency without sacrificing reliability. TPC schemes typically adopt a closed loop system architecture as shown in Fig. 1. In this system, the sink node receives the data packet from the sensor node and measures the RSSI at each transmission cycle. According to the measured RSSI value, the next transmission power level is calculated and such information is feedback to the sensor node using a control packet. Then, the sensor node can update the current transmission power level according to the feedback information. The above procedures repeat at each transmission cycle during the lifetime of the nodes, thus the sensor node can adapt its transmission power level in the run-time to the channel condition.

There are four most representative studies [6], [7] regarding TPC in WBAN. Xiao *et al.* in [6] propose a real-time reactive scheme under the off-body channel condition. This scheme measures an average RSSI value according to each received data packet. By comparing the average RSSI value to a predefined threshold, the real-time reactive scheme accordingly adjusts the TPL. This study was the first to implement adaptive power control in WBAN. However, the proposed scheme is not tested in an on-body channel whose channel fluctuation is larger than that of the off-body channel.

The dynamic postural position inference (DPPI) mechanism which performs adaptive body posture inference for optimal power assignments is presented in [9]. DPPI is specific to the on-body channel condition. It first measures the linear relationship between the TPL and RSSI by sending control packets, and then calculates a desirable TPL. The DDPI scheme can quickly converge to the desire TPL. However, this approach is not practical if the user is in continuous motion.

Kim *et al.* in [8] found that in cases where interference was present, RSSI is not a correct indicator to determine the link

state. They proposed a practical scheme which uses the RSSI and link quality indication (LQI) to distinguish between attenuation and interference. This scheme not only controls transmission power but also avoids interference. To control the transmission power, the proposed scheme uses a weighted average value to indicate the link state. The experimental results show that the proposed protocol has high energy efficiency and reliability in the presence and absence of interference.

The scheme proposed in [7] uses short- and long-term link-state estimations. The short-term link-state estimation was designed to quickly adapt the transmission power, and the long-term link-state estimation is used to stabilize the link state in the variable link state.

In addition to optimizing the transmission power, studies in [10] and [11] focus on the energy consumption of receiving control packets from the sink node. The studies point out that the energy consumption of the receiving of control packets should not be neglected and they discuss the methods for adaptively adjusting the feedback periodicity based on the current channel environment. Lee *et al.* in [12] present an algorithm that can adaptively select conservative or aggressive control mechanisms depending on the current channel condition. Zhang in [13] investigates the energy saving efficiency of transmission power control and link adaption, and points out that link adaption can outperform transmission power control under a certain condition.

Because of periodic movements of the human body, dynamic WBAN wireless channels always present a unique periodicity characteristic that differs from other kinds of wireless channels. Roberts *et al.* in [4] investigate the periodicity characteristic of dynamic WBAN channels and propose a new channel model involving these periodicity characteristics. They found that if the channel periodicity could be fully exploited, the radio receiving sensitivity threshold could be significantly increased, resulting in large power savings. Prabh *et al.* in [5] use channel periodicity to arrange the transmission time of WBAN nodes under ideal channel conditions. This scheme works on the Media Access Control (MAC) layer, and intermittently broadcasts a chain of probing packets to estimate the RSSI period, which introduces additional traffic along with extra energy consumption. Zang *et al.* in [14] exploit periodic body movements to reinforce the transmission power control scheme in dynamic channel conditions. However, their work is specific to a sensor node worn on the wrist.

III. Periodic Link State Fluctuation

In this section, we present the investigation of the periodic fluctuation of on-body wireless link state (in terms of RSSI) in walking scenario through the experiment. We use real world measurements. Both the RSSI and acceleration signal are collected at the sink node at a sampling rate of 50 Hz. They are synchronized in time and input into a laptop via a long wire. A person holds the laptop, allowing the participant to move freely. All the measurements are analyzed on the laptop using Matlab. Our study uses a platform with a CC2420 radio [15]. The CC2420 is a true single-chip 2.4 GHz IEEE 802.15.4 compliant RF transceiver designed for low power and low voltage wireless applications. CC2420 includes a digital direct sequence spread spectrum baseband modem providing a spreading gain of 9 dB and an effective data rate of 250 kbps. CC2420 supports 31 transmission power levels that can be dynamically controlled during run-time via a register. Table I shows the typical energy consumption of CC2420. Our platform also has a three-axis accelerometer (Freescale MMA8451Q [16]), which is used to monitor acceleration signals at the sink node. It is a smart micro-machined accelerometer with a 14 bit resolution to the x-,y-,z-axis and supports $\pm$2g, $\pm$4g, and $\pm$8g dynamically selectable measurement ranges. The MMA8451Q sampling rate is programmable. Six subjects (age 24.4 $\pm$ 6.05 years, height 170.2 $\pm$ 5.3 cm, and body mass index 21.1 $\pm$ 3.3 kg/m^2. three females and three males) were recruited to participate in the experiment.

TABLE I
Specifications of the CC2420 Radio [15]

Transmit level	Power (dBm)	Consumption (mW)
31	0	31.3
27	−1	29.7
23	−3	27.4
19	−5	25.0
15	−7	22.5
11	−10	20.2
7	−15	17.9
3	−25	15.3

When the WBAN user is walking, the on-body wireless link state fluctuates as the sensor nodes move along with body movements. Body movements during walking are usually periodic, making the resultant link state fluctuations periodic. Fig. 2 illustrates a 10 seconds snapshot of logged RSSI of ankle to pants pocket (Fig. 2(a)) and ankle to waist (Fig. 2(b)) deployment. Both RSSI traces exhibit a clear periodic fluctuation. These channel fluctuations are not only periodic but also time-synchronized with the gait cycle. This can be explained as following. The subjects legs swing back and forth during walking; when the leg with the senor node swings to the front of the torso, the channel is line-of-sight (LOS), resulting in a RSSI peak. During the rest of the gait cycle, the wireless link is blocked by the torso. The deepest channel attenuation occur when another leg swings to the front of the torso leaving the transmitter completely behind the torso. The channel fluctuation produced at other deployments such as wrist to chest or pants pocket to chest are also periodic and time-synchronized with the gait cycle for similar reasons.

As discussed above, the channel fluctuations are periodic and time-synchronized with the gait cycle in many deployments. Therefore, the RSSI peaks can be predicted by analyzing the gait cycle information. If transmission occurs at the RSSI peaks rather than the valleys, approximately 20 dB[1] power can be

[1]In our experiment, the channel fluctuation (defined as the value difference from the RSSI valleys to the RSSI peaks) is more than 20 dB from the limbs to the torso. When the sensor node is closer to the sink such as from pant pocket

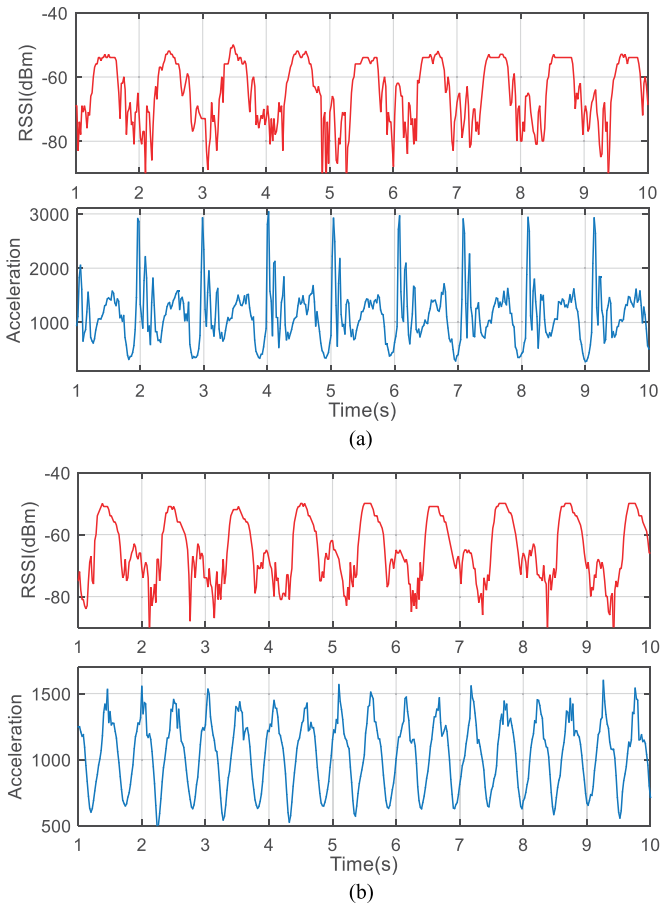

Fig. 2. 10 seconds snapshot of measured RSSI and acceleration signal while subject is walking with node deployment of: (a) ankle to pants pocket, (b) ankle to chest.

saved. Periodic channel fluctuation allows us to always find the RSSI peaks to arrange transmissions.

To present the gait cycle, the acceleration signal was collected from an accelerometer on the sink node. To eliminate the effect of different sink node orientation, we use the signal magnitude vector of acceleration, La, which is insensitive to orientation. La is calculated as:

$$La = \sqrt{La_x^2 + La_y^2 + La_z^2} \tag{1}$$

here La_x, La_y and La_z are the acceleration signal at x-axis, y-axis and z-axis. As can be seen in Fig. 2, the acceleration signals present a certain oscillation. When the sink node is in the pants pocket, the acceleration signal reflects the movement of the leg with the accelerometer (as shown in Fig. 2(a)). The peaks in the acceleration signal correspond to the moments when the heel strikes the ground, and follow the stance and swing phase of the leg. When the sink node is located at the chest, the acceleration signal reflects the movement of the torso (as shown in Fig. 2(b)). This acceleration signal shows a sequence of peaks and valleys since the body experiences a series of upward and downward movements during walking. All of the different kinds of acceleration signals contain the gait cycle information. Gait analysis is a well-researched field, interested readers can refer to [17] for more comprehensive information.

to chest, the corresponding channel fluctuation is about 10 dB. When both the sensor node and the sink are on the torso, the corresponding channel fluctuation is insignificant. Although the proposed scheme is general and applicable to many different node placements, this study primarily focuses on the channel from the limbs to torso as it poses a major TPC challenge.

IV. Methods

In this section, we introduce the gait cycle driven transmission power control (G-TPC) scheme including the system structure, user state detection, gait cycle tracking, RSSI peak location and transmission power determination.

A. System Overview

There are three main states in G-TPC: *Original TPC*, *Self-learning* and *Transmission*. Initially, if the user is stationary, the system enters the *Original TPC* state, otherwise it enters the *Self-learning* state. The user state (walking or stationary) is distinguished by the user state detection procedure. In the *Original TPC* state, G-TPC sends the data packets in the conventional TPC fashion without any transmission time scheduling. But if the user state changes to walking, the system immediately enters the *Self-learning* state. The objective of the *Self-learning* state is to learn the relationship between the gait cycle and the time points of the ideal channel condition. In the *Self-learning* state, the gait cycle tracking procedure, aiming at capturing each stride, begin to work and the RSSI peak location procedure is carried out to find the optimal transmission point (RSSI peak) in a stride. Subsequently, the system leaves the *Self-learning* state and enters the *Transmission* state in which G-TPC scheme sends data packets at the scheduled transmission times with the transmission power level adjusted by analyzing the RSSI feed-backed from the receiver. In the *Transmission* state, the gait cycle tracking procedure continues to work providing the reference points for scheduling the transmission time points. If the transmission power level fluctuates across five consecutive transmission cycles, indicating the failure of the transmission time scheduling, the system returns to the *Self-learning* state to repeat gait cycle tracking and the RSSI peak location procedure. If the transmission time scheduling still fails, indicating the related channel is not periodic or is periodic but not time-synchronized with the gait cycle, the system goes to the *Original TPC* state. The system runs on the sink node, so the information regarding transmission times and transmission power is sent back to the transmitter with the help of the control packets. The state diagram of G-TPC is illustrated in Fig. 3.

In our scheme we use an accelerometer to obtain the user gait cycle information and recognize the user state. The accelerometer is only required at the sink node. There is no restriction on the physiology sensor at the sensor node.

B. User State Detection

To detect the user state, this study uses a lightweight online recognition method using acceleration signals [18]. The acceleration signals are collected on the sink node and smoothed by

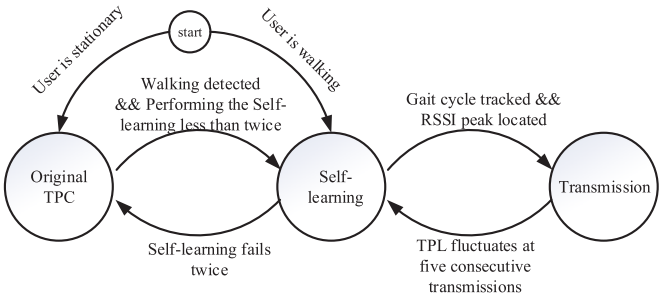

Fig. 3. State diagram of G-TPC scheme.

an order 3 median filter. The filtered signals are segmented in real time using a sliding window with 2-second size and a 1-second shift between the consecutive windows. Therefore, the user state is detected every second.

Because walking produces a large fluctuation in the acceleration signal, the first-order regression coefficient is calculated on the acceleration samples in the sliding window as:

$$f(n) = \frac{(La(n+1) - La(n-1)) + 2 \cdot (La(n+2) - La(n-2))}{2 \cdot (1^2 + 2^2)} \tag{2}$$

where La is the acceleration sample in the sliding window. The next step is to extract the mean absolute deviation (MAD) of the values obtained as :

$$MAD = \frac{1}{L-4} \sum_{\tau=t_w-L-1}^{t_w} |f(\tau) - \mu| \tag{3}$$

where t_w denotes the time index of the current sliding window, μ is the mean value of the $f(n)$ in the sliding window and L is the sliding window length. The MAD presents an excellent feature for differentiating the motion and motionless user states. When the user is motionless (sitting or standing), the MAD is close to 0 and it increases to more than 100 when the user starts to walk. A threshold of 50 is adopted in the proposed scheme. If the MAD is higher than this threshold, the current user state is recognized as in motion; otherwise, it is recognized as motionless. Fig. 4 illustrates an example of the user state detection. The study in [18] shows that this method has approximately 95% accuracy. Therefore, we believe that errors in classifying user state have negligible effects on the overall performance of our scheme.

C. Gait Cycle Tracking and RSSI Peak Location

As previously mentioned, the periodic channel fluctuation and gait cycle are usually synchronized in time, thus the time instance of the ideal channel can be predicted by analyzing the acceleration signals. To achieve this, the proposed scheme must track the on-going gait cycles and obtain the RSSI peaks location in each stride. Moreover, the gait cycle tracking and RSSI peak location can be applied to any oscillation pattern in the acceleration signal due to variations in sink node locations and the users walking habits.

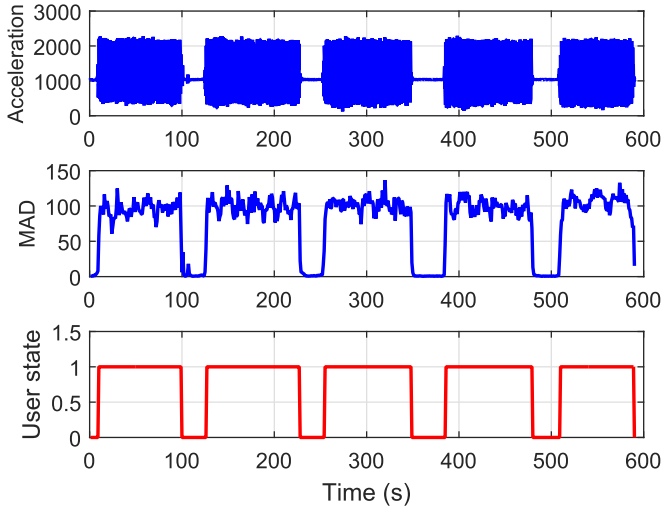

Fig. 4. An example of the user state detection method. The MAD (second row) is calculated on the real time collected acceleration signals (first row). The corresponding user state detection results indicated by "1" (motion) or "0" (motionless) are shown at the third row.

Algorithm 1: Template Generation.

Require: the user activity is walking for 3 seconds.
Input:
1: Acc_seg: vector of acceleration of the nearest two seconds
2: $Length$: the length of acceleration template
3: $Index$: the index of a maximum point
Output:
4: $Template$: vector of acceleration template
Begin
5: $Acc\_seg \leftarrow$ average moving filter (Acc_seg)
6: $Index \leftarrow argmax_i \{Acc\_seg\,(end - 50 : end)\}$
7: $Template \leftarrow Acc\_seg\,(index - Length - 1 : index)$
End

In the proposed scheme, a template matching method is adopted to track the gait cycle in real time. The acceleration template is generated one second after the user state is recognized as in motion. Waiting for one second ensures that the motion is stable. To guarantee the accuracy of template matching, the template length is set as 1.6 seconds and an extreme point (local maximum) is chosen as the end point of the template. The algorithm of template generation is shown in Algorithm 1.

A stride point is defined as the point in time where the template is found very similar to a part of the real time acceleration signal. By detecting the time point of each stride, the system can effectively track the on-going gait cycle. The user may change walking speed, causing variations in stride length. Thus, some certain popular similarity measures, such as Euclidean Distance and Cross Correlation which require that two sequences have the same size, has poor efficiency in this application. Instead, Dynamic Time Warping (DTW) which has long been known in the speech processing community, can be used to measure the similarity between two sequences that may spread or compress in time. A variation of DTW is subsequence DTW

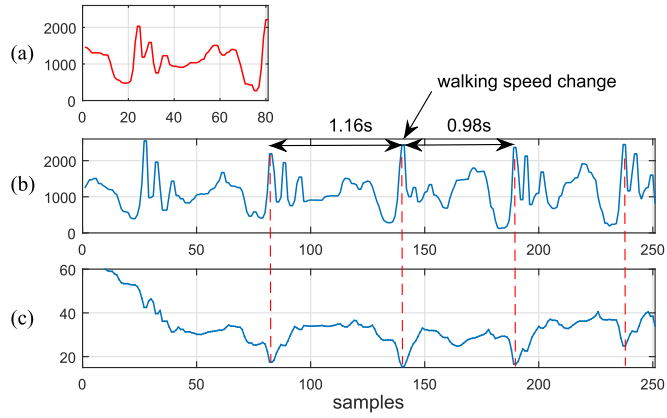

Fig. 5. (a) Acceleration template. (b) Acceleration samples of four strides collected by the accelerometer at the users pants pocket. Note that the walking speed increases from 1.16 seconds per stride to 0.98 seconds at the second stride. (c) Template distance values corresponds to the top row of the accumulated cost matrix C. The red dash lines indicate that local minimums in distance values correspond to stride points even when the stride length changes.

(sDTW) [19], which is used to locate a subsequence within a longer sequence that optimally fits the template. In our study, the sDTW is implemented to locate a subsequence of the real time collected acceleration signal which is similar to the template signal.

Suppose an acceleration template of length n have been generated, and the real time acceleration signal of length m is collected as the user is walking. We use time series Q and S to represent the template signal and real time acceleration signal respectively, as: $Q = q_1, q_2, \ldots, q_i, \ldots, q_n$ and $S = s_1, s_2, \ldots, s_i, \ldots, s_m$. The sDTW algorithm constructs an n-by-m distance matrix d, where each element (i, j) contains the Euclidean distance $d(q_i, s_i)$ between two points q_i and s_i. A warping path is a set of cost matrix elements that defines a mapping between Q and S with an accumulated cost. An optimal warping path has the lowest accumulated cost among all possible choices. This path can be found efficiently using dynamic programming. To do this, an accumulated cost matrix C, which represents the accumulated costs of warping the template to parts of a real time acceleration signal, is built from the distance matrix d as follows. The first column and the last row of matrix C are built as $C(i,1) = \sum_{k=1}^{i} d(q_k, c_1),\ \forall i \in \{1, \ldots n\}$ and $C(n,j) = d(q_1, s_j),\ \forall j \{1, \ldots m\}$, and the remaining elements are calculated using the recursive function: $C(i,j) = \min\{C(i-1,j-1) + C(i-1,j) + C(i,j-1)\} + d(q_i, s_i), \forall i \in \{1, \ldots n-1\}, j \in \{1, \ldots m-1\}$.

The first row of the accumulated cost matrix C is the total accumulated cost for warping template Q to each point in real time acceleration signal S. Therefore, the local minimums of the first row of C can be used to indicate the stride point. Fig. 5 shows an example of locating the stride point using sDTW.

In our scheme, a sliding window is used to hold the acceleration samples. Every 20 ms (the time interval of the acceleration sample), a new acceleration sample is input into the sliding window, while the oldest one is dropped. The window length is set as 2 seconds so one entire template (1.6 s) can be covered. Gait cycle tracking is realized by performing the sDTW between the acceleration samples in the sliding window with the template at every 80 ms time step. A small time step, i.e. 20 ms (the time interval of one acceleration sample), increase the computation load, while a large time step cannot properly seize each stride. In our study, we empirically set the time step as 80 ms. As mentioned, the sDTW algorithm is used to measure the similarity and produces an accumulated cost matrix C. A minimum point p_0 can be found in the first row of matrix C as $p_0 = \arg\min_i \{C(1,:)\}$, where i is the element index in $C(1,:)$. There are some random dips around the minimum point, resulting in false minimum point detection. In the gait cycle tracking algorithm, we use the condition $15 < \arg\min_i (C(1,:)) < 85$ to ensure that the minimum point is fully covered by the sliding window. This guarantee the accuracy of the algorithm. The time point of current stride can be obtained according to the start-time of the slide window. Consequently, the stride period can be calculated as the time interval

Algorithm 2: Gait Cycle Tracking.

Input:
$Temp\_acc$: vector of acceleration template
T_s: time interval of acceleration samples
Win_acc: slide window for holding the acceleration samples
T_{dtw}: the time point of performing sDTW
$T_{current}$: the current time point

Output:
T_{str}: the time point of current detected stride
$T_{str}^{'}$: the time point of last detected stride
C: resulted accumulated cost matrix from sDTW algorithm
$current\_stride\_period$: the current stride period

Begin
$T_{dtw} \leftarrow$ time point of the last sample in acceleration template + 500 ms
while receive an acceleration sample **do**
  $Win\_acc \leftarrow \{newsample, Win\_acc(2:end)\}$
  if $T_{current} == T_{dtw}$ **then**
    $C = sDTW(Temp\_acc, Win\_acc)$
    if $T_c < T_{dtw} + (\arg\min_i (C(1,:)) - length(Win\_acc)) \times T_s - 700\,\text{ms}\&\&15 < \arg\min_i (C(1,:)) < 85$ **then**
      $T_{str}^{'} \leftarrow T_{str}$
      $T_{str} \leftarrow T_{dtw} + (\arg\min_i (C(1,:)) - length(Win\_acc)) \times T_s$
      $stride\_period \leftarrow T_{str} - T_{str}^{'}$
      $T_{dtw} \leftarrow T_{dtw} + 80\,\text{ms}$
    else
      $T_{dtw} \leftarrow T_{dtw} + 80\,\text{ms}$
    end if
  end if
end while
End

between the last and current stride point. The gait cycle tracking procedure is summarized in Algorithm 2.

Since the RSSI peak has an arbitrary phase between two adjacent stride points, the RSSI peak location in the stride period (defined as the period between two adjacent stride points) must be estimated after the gait cycle is tracked. To this point, the transmitter sends probing packets to the sink node at a frequency of 25 Hz for one stride period. At the sink node, we apply a moving average filter of order 3 on the collected RSSI sample to remove the noise. A maximum value is located on the filtered signal. To enhance the G-TPC robustness, the RSSI peak location is defined as the center point of the RSSI peak formed by the samples with value higher than 80% of the RSSI maximal value in a stride period. After determining the corresponding RSSI peak area, the RSSI peak location is decided. It should be noted that this location is defined as a ratio with respect to the stride period, and remains unchanged at different walking speeds. For example, suppose a RSSI peak location is 25% of a stride period. If the stride period is 1000 ms, the RSSI peak is then located at the $1000 \times 25\% = 250$ ms away from the stride point. If the walking speed is increased, making the stride period shorten to 900 ms, the system automatically updates the RSSI peak location according to the new stride period ($900 \times 25\% = 225$ ms away from the beginning of the stride). The system can always track the users gait cycle. Therefore, the system is able to predict the beneficial transmission time points with the RSSI peak location information.

The RSSI peak locating procedure introduces additional energy consumption since some control packets are transmitted. This procedure is performed only one or two times if the node placement remains unchanged, making the energy consumption negligible when compared to the overall energy consumption of the WBAN node. For this reason we do not consider the energy consumption of the RSSI peak locating procedure in this study. The use of the sDTW algorithm incurs an approximately 300 ms computation lag in our scheme (because of the condition $15 < \arg\min_i (C(1,:)) < 85$ in the gait cycle tracking procedure). Thus the next transmission time point is actually derived from the gait cycle information of the last stride. Because the people tend to walk at certain speed for a period of time, the computation lag does not have a significantly negative effect on G-TPC.

D. Transmission Power Determination

At the point when the on-going gait cycle is being tracked and the RSSI peak location has been obtained, the sink node is then capable of predicting the beneficial transmission time points by monitoring the local acceleration signals. Since all algorithms are running on the sink nodes, the information of the predicted transmission time point of the next packet is sent back to the transmitter with the control packet at each transmission cycle. The transmitter can transmit the packets at these time points with the transmission power determined as follow.

At each transmission time, the transmission power level is determined by the feedback information from the receiver as in RSSI/LQI Based Transmission Power Control (RL-TPC) [8]. First, the current channel state is evaluated by calculating the weighted average RSSI, denoted as $E[x]$, of the n latest samples in (4) as:

$$E[x] = \frac{w(x_1)\cdot x_1 + w(x_2)\cdot x_2 + \cdots + w(x_n)\cdot x_n}{w(x_1) + w(x_2) + \cdots + w(x_n)} = \frac{\sum_{i=1}^{n} w(x_i)\cdot x_i}{\sum_{i=1}^{n} w(x_i)} \tag{4}$$

where x_i represents the RSSI value of the i-th sample in a received sequence including n latest samples. A smaller i represents a more recently received value and $w(x_i) = \alpha^{i-1}$ is the weighting coefficient of x_i indicating that the more recent samples are weighted heavier than the older samples. The calculated $E[x]$ is compared to the predefined target threshold, since it is an appropriate indicator that reflects the current channel state in dynamic scenarios. A target margin bound by the upper and lower threshold must be set. If the resulting $E[x]$ is higher than this upper threshold, the transmitter decreases the power level by α_{down}. Likewise, if $E[x]$ is less than the lower threshold, the power level is increased by α_{up}. The output power remains unchanged if the $E[x]$ is within this target margin. The values of α_{up} and α_{down} are set to 1 and 3 in this study.

It should be noted that the channel fluctuation at some node deployments is not periodic or the periodic fluctuation is not time-synchronized with the gait cycle. Further, the RSSI peak location procedure may not extract the correct location. If either of these situations occurs, the adjusted transmission power is not able to be kept stable. Therefore, if the transmission power levels keep fluctuating across five consecutive transmission cycles, the system performs the RSSI peak location procedure again. If the transmission power levels still cannot be kept stable after the procedure is performed two times, the system adopts the conventional transmission power control scheme without performing transmission times scheduling.

The proposed scheme can have the adverse impact of an increase in buffer delay since the system needs time to perform the on-line learning procedure and the buffered packets need to wait for the scheduled transmission time. To reduce this adverse impact, when its waiting time exceeds a certain threshold the packet is forced to transmit using the conventional TPC protocol. According to the latency requirement in ISO/IEEE 11073 Draft for Point-of-Care (PoC) medical devices [20], the threshold is set as 3 seconds. Further, if there are more than two packets at the buffer, two packets are sent sequentially to the sink at the scheduled time. It is possible to send at least two packets at one RSSI peak point because the RSSI signal resides at a high level (no less than 90% of the peak value) for about 15 ms while the airtime of a completed communication is less than 5 ms.

V. Experiment Results and Performance Evaluation

In this section, we evaluated the performance of the proposed G-TPC in an experiment. For the performance evaluation, we considered a WBAN where the sensor node is attached on the ankle and transmits the sensory data to the sink node placed on the subject's pants pocket. We chose this node placement for evaluation since it best addresses the challenge of rapid dy-

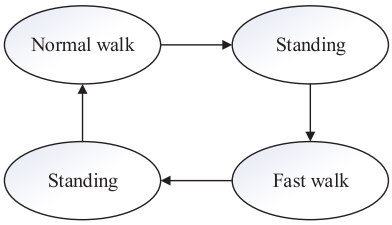

Fig. 6. Activity pattern used in the experiment.

TABLE II
MEAN GAIT CYCLE TIME (SECOND)

	Normal walk case	Fast walk case
Subject 1	1.076	0.967
Subject 2	1.140	1.061
Subject 3	1.034	0.967
Subject 4	1.31	1.140
Subject 5	1.035	0.957
Subject 6	1.085	0.990

namic channel fluctuation. The experiment setup is introduced in Section III. On a computer, Matlab was used to analysis the collected data.

In the experiment subjects carrying the WBAN nodes were asked to walk on a pedestrian footpath in a prescribed activity pattern shown in Fig. 6. The activity pattern consisted of 60 seconds of walking at a normal speed (5 km/hour), 10 seconds of standing, 60 seconds of fast walking (6 km/hour) and 10 seconds of standing. This pattern was repeated six times in one test, which lasted approximately 20 minutes. Each subject was asked to perform the test twice. This resulted in approximately 4 hours of data including 12332 strides in total (The strides are manually labeled and the mean gait cycle time are summarized in Table II). In this study, data packets were generated every second. In the original RL-TPC the sensor node sends a data packet when it is generated, resulting in a one second transmission cycle. During each transmission cycle, the sink node determines the next TPL and a control packet is fed back to the sensor node with the TPL information. In the proposed G-TPC scheme, the sink node determines the transmission time and feeds it back to the sensor node if the user is walking. At the sensor node, the generated data packets are first held in buffer and are transmitted at the scheduled time. If the user state is static, the G-TPC scheme operates in conventional fashion as the original RL-TPC. The target RSSI threshold range is set as -85 dBm and -80 dBm in both cases.

We use the following error measurement criteria to evaluate the accuracy of stride point detection in the gait cycle tracking procedure. The *false positive rate (FPR)* is computed as the percentage of total number of false detected stride points (the detected stride points which are not the true ones) out of the total number of manually labeled stride points (gold standard):

$$FPR = \frac{\sum \text{false detected stride points}}{\sum \text{labeled stride points}} \tag{5}$$

Similarly, the *false negative rate (FNR)* is computed as the percentage of the number of undetected stride points (the true stride points which are missed by gait cycle tracking procedure) out of the total number of manually labeled stride points

$$FNR = \frac{\sum \text{undetected stride points}}{\sum \text{labeled stride points}} \tag{6}$$

TABLE III
ERROR MEASUREMENT RESULTS OF STRIDE POINT DETECTION

	FPR	FNR
Subject 1	0.24%	3.6%
Subject 2	0.21%	4%
Subject 3	0.19%	3%
Subject 4	0.2%	4.2%
Subject 5	0.24%	3.3%
Subject 6	0.25%	4%

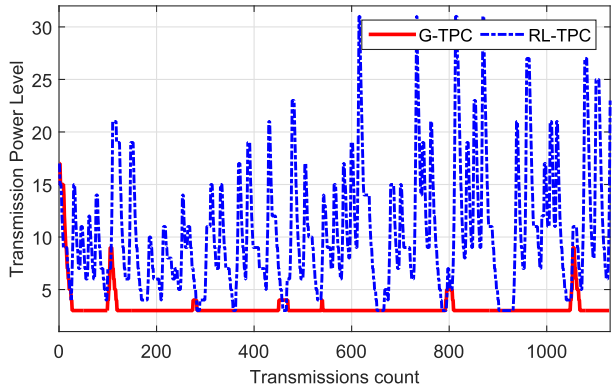

Fig. 7. Transmission power levels of the original RL-TPC and G-TPC.

The error measurement results are summarized in Table III, From this table we observe that the FPR and FNR is lower than 0.25% and 4.2%, according to the performance evaluation of packet loss rate and power consumption per packet on sensor node (are introduced later), the accuracy of the stride point detection is sufficient for the proposed G-TPC scheme.

Fig. 7 shows the transmission power levels of RL-TPC and G-TPC of subject 1. The rest of the results are similar and are omitted here. The transmission power levels of RL-TPC drastically fluctuate between 3 and 31 due to the unstable wireless link. For RL-TPC, the current link state is obtained by probing the channel with data packets and then adjusts the transmission power according to the current link state. Therefore the channel coherent time must be much longer than the interval of the transmission times. However, in the walking scenario, the on-body wireless channel fluctuates quickly and drastically (especially when nodes are deployed on the ankle or on the wrist), and the feedback packets fail to reflect the rapidly varying link states in real time, causing invalid transmission power adjustments. Moreover, even if RL-TPC can track the channel variations, high transmission power levels are also necessary when the packets are transmitted at a poor point of the varying channel.

Most of the time the transmission power levels of G-TPC are at the lowest level. The TPL only rises at transitions between user states and the TPL decreases quickly when the user state is stable. In order to make a fair comparison, we also calculate the

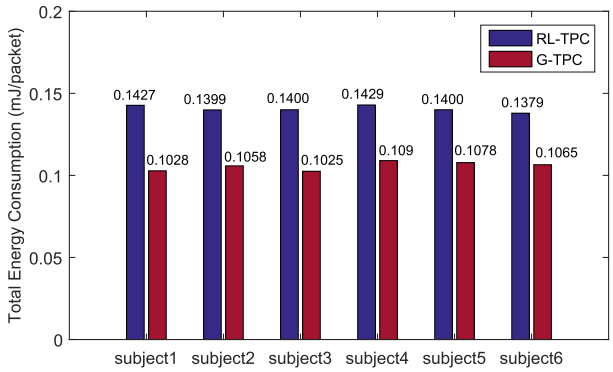

Fig. 8. Energy consumption of the original RL-TPC and G-TPC on the sensor node.

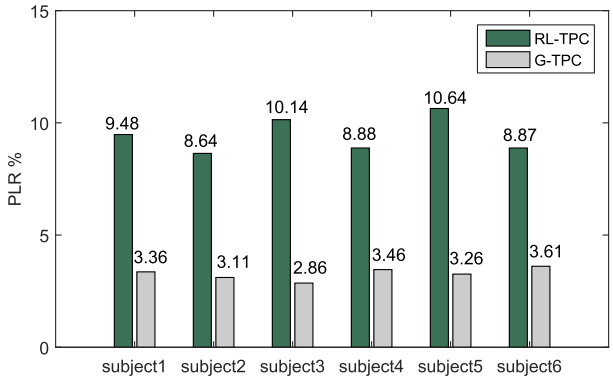

Fig. 9. Packet loss rate of the original RL-TPC and G-TPC.

energy consumption (in terms of mJ/packet) on the transmitter side for successful delivery of one data packet, based on the power consumption of various transmission power levels presented in Table I. The length of the data packet is set at 128 Bytes and the data rate is 250 kbps. The calculation of energy consumption is only for the sensor node alone since the object of the power control scheme is to save the battery power of the sensor node. This is due to the fact that the sensor nodes battery capacity is typically small because of the miniaturization requirement and the need to operate for a long period of time, while the sink node always has large battery capacity and thus has less of an energy constraint. The packet loss is calculated to evaluate the reliability. There is no well-accepted symbol error probability model for this communication scenario. To give a better performance evaluation to the proposed scheme in this study we chose a RSSI threshold of -90 dBm to calculate the packet loss by referring to the experimental results published in [7]. Specifically, the packet loss number is the number of packets whose RSSI is lower than -90 dBm [11]. The results of the comparison of energy consumption and PLR between RL-TPC and G-TPC are shown in Figs. 8 and 9. The average PLR of 6 subjects is 3.28% and 9.44% in G-TPC and RL-TPC, respectively. The average sensor node energy consumption of 6 subjects is 0.1057 mJ/packet and 0.1406 mJ/packet in G-TPC and RL-TPC, respectively. Thus, compared to the original RL-TPC, G-TPC reduces energy consumption by 25% on the sensor node and reduce packet loss rate by 65%.

TABLE IV
BUFFER DELAY OF SIX SUBJECTS IN G-TPC

	Buffer delay (second)
Subject 1	0.92
Subject 2	0.98
Subject 3	0.85
Subject 4	1.12
Subject 5	0.88
Subject 6	0.97

In the proposed scheme, the extra power consumption on the sink node is in collecting the acceleration signal, which is 0.06 mw (Freescale Semiconductor [16]). Consider the average power consumption saving for the sensor node is (0.1406 – 0.1057) mJ/packet = 0.0349 mw in our experiment, more power is consumed on the sink node. However, the sink node usually has more energy resource than sensor node, take the smart phone as example, the battery capacity is usually more than 3000 mAh (37.8 kJ). If the accelerometer operates 8 hours per day, total 1.152 J energy (0.06 mw $\times$ 8 $\times$ 60 $\times$ 60 s) is consumed, which takes a tiny portion of the battery capacity. So the power consumption on the sink node introduced by the proposed scheme has negligible impact to recharge time interval of the sink node. Moreover, if the sink node already has application which requires the acceleration signal, (such as fall detection, abnormal movement detection, pedometer, energy expenditure estimation and human activity detection, etc.), the proposed scheme can take advantage of the existing acceleration signal for free.

VI. A DISCUSSION OF THE BUFFER DELAY AND THE COMPUTATIONAL LOAD IN G-TPC

G-TPC scheme has demonstrated good performance with respect to PLR and energy consumption. However, this causes a buffer delay and computational cost. There are two reasons for the buffer delay introduced by G-TPC scheme: 1) a set-up time is required for the gait cycle tracking operation; 2) the transmitter only sends packets at the most beneficial time point in each stride (while the conventional TPC sends packets immediately). The average buffer delays of the six subjects using G-TPC are shown in Table IV. G-TPC scheme restricts the buffer delay below a predefined threshold by the mechanism described in Section IV.

The computation load is dominated by the sDTW calculation we used to track the gait cycle. The time complexity of sDTW is $O(MN)$ where M and N are the length of the sliding window and the acceleration template, respectively. In the proposed scheme, we set M as 96 and N as 80, leading to a time complexity of $O(7680)$. The gait cycle tracking should be applied in the sink node which has powerful computing ability and large battery capacity. The energy savings we consider is only related to the sensor node which has a small battery capacity due to miniaturization and is required to operate for a long time. We provide two suggestions as follow to reduce the computation load if the device being used cannot meet the requirements of the computation complexity.

1) Adopting a Modified DTW: An algorithm named Piecewise Dynamic Time Warping (PDTW) [21], takes advantage of the fact that most time series can be efficiently approximated by a piecewise aggregate approximation, can be adopted to speeds up the computation. The time complexity for PDTW is $O(MN/c^2)$, where c is the ratio of the length of the original time series to the length of its piecewise aggregate approximation. A speedup of $O(c^2)$ is thus obtained.

2) Performing the Gait Cycle Tracking in a Longer Time Interval: To achieve the best performance, in this study we perform the gait cycle tracking operation every 80 ms. Considering that people tend to walk at certain speed for a period of time, the gait cycle tracking operation can be triggered only when the TPL is not stable at the low level, to calibrate the transmission time points.

VII. Conclusion

In WBAN, body movements can result in rapid dynamic channel conditions and severely degrade the performance of conventional TPC schemes. To remedy this problem, G-TPC exploits the periodicity characteristic of body movements to predict the time points of ideal channel conditions in walking scenario by using the gait cycle information. This results in significant reductions in the transmission power. When the user is motionless, G-TPC operates as a conventional TPC scheme, since it is sufficient for motionless scenarios. To better evaluate the performance, a combination scenario that include both walking (at different speeds) and standing was considered in our experiment. The results reveal that energy consumption can be reduced by 25% on the sensor node and the packet loss rate can be reduced by 65% compared to the original RL-TPC. Future work in this area should include extending this scheme to other daily activities like running and ascending/descending stairs.

References

[1] R. Cavallari, F. Martelli, R. Rosini, C. Buratti, and R. Verdone, "A survey on wireless body area networks: technologies and design challenges," *IEEE Commun. Surveys Tuts.*, vol. 16, no. 3, pp. 1635–1657, Feb. 2014.

[2] M. Patel and J. Wang, "Applications, challenges, and prospective in emerging body area networking technologies," *IEEE Trans. Wireless Commun.*, vol. 17, no. 1, pp. 80–88, Feb. 2010.

[3] C. He, X. Fan, and Y. Li, "Toward ubiquitous healthcare services with a novel efficient cloud platform," *IEEE Trans. Biomed. Eng.*, vol. 60, no. 1, pp. 230–234, Oct. 2013.

[4] N. E. Roberts, S. Oh, and D. D. Wentzloff, "Exploiting channel periodicity in body sensor networks," *IEEE J. Emerg. Sel. Topics Circuits Syst.*, vol. 2, no. 1, pp. 4–13, Mar. 2012.

[5] K. S. Prabh, F. Royo, S. Tennina, and T. Olivares, "BANMAC: an opportunistic mac protocol for reliable communications in body area networks," in *Proc. IEEE 8th Int. Conf. Distrib. Comput. Sensor Syst.*, May 2012, pp. 166–175.

[6] S. Xiao, A. Dhamdhere, V. Sivaraman, and A. Burdett, "Transmission power control in body area sensor networks for healthcare monitoring," *IEEE J. Sel. Areas. Commun.*, vol. 27, no. 1, pp. 37–48, Jan. 2009.

[7] S. Kim and D.-S. Eom, "Link-state-estimation-based transmission power control in wireless body area networks," *IEEE J. Biomed. Health Informat.*, vol. 18, no. 4, pp. 1294–1302, Jul. 2014.

[8] S. Kim, S. Kim, and D.-S. Eom, "RSSI/LQI-based transmission power control for body area networks in healthcare environment," *IEEE J. Biomed. Health Informat.*, vol. 17, no. 3, pp. 561–571, May 2013.

[9] M. Quwaider, J. Rao, and S. Biswas, "Body-posture-based dynamic link power control in wearable sensor networks," *IEEE Commun. Mag.*, vol. 48, no. 7, pp. 134–142, Jul. 2010.

[10] B. Moulton, L. Hanlen, J. Chen, G. Croucher, L. Mahendran, and A. Varis, "Body-area-network transmission power control using variable adaptive feedback periodicity," in *Proc. IEEE Aust. Commun. Theory Workshop*, 2010, pp. 139–144.

[11] G. Yi, D. Yu, and N. Kim, "Adjusting control packet transmission intervals in low power sensor systems," *Int. J. Distrib. Sens. Netw.*, vol. 2014, Aug. 2014.

[12] W. Lee, B.-D. Lee, and N. Kim, "Hybrid transmission power control for wireless body sensor systems," *Int. J. Distrib. Sens. Netw.*, vol. 2014, Oct. 2014.

[13] Q. Zhang, "Energy saving efficiency comparison of transmit power control and link adaptation in BANs," in *Proc. IEEE Int. Conf. Commun.*, Jun. 2013, pp. 1672–1677.

[14] W.-L. Zang, S.-L. Zhang, and Y. Li, "An accelerometer-assisted transmission power control solution for energy-efficient communications in WBAN," *IEEE J. Sel. Areas. Commun.*, vol. 34, no. 12, pp. 3427–3437, Dec. 2016.

[15] Texas Instruments, CC2420 Datasheet, Jun. 2004. [Online]. Available: http://www.ti.com

[16] Freescale Semiconductor, MMA8451Q, May 2012. [Online]. Available: http://www.freescale.com.

[17] C. Soaz and K. Diepold, "Step detection and parameterization for gait assessment wsing a single waist-worn accelerometer," *IEEE Trans. Biomed. Eng.*, vol. 63, no. 5, pp. 933–942, Sep. 2015.

[18] O. Yurur, C. H. Liu, and W. Moreno, "Light-weight online unsupervised posture detection by smartphone accelerometer," *IEEE Internet Things J.*, vol. 2, no. 4, pp. 329–339, Aug. 2015.

[19] M. Muller, *Information Retrieval for Music and Motion*. Berlin, Germany: Springer, 2007.

[20] *Draft Health Informatics—Point-of-Care Medical Device Communication—Technical Report—Guidelines for the Use of RF Wireless Technology*, IEEE Unapproved draft Std P11073–00101/D5, Jun. 2008.

[21] E. Keogh and M. Pazzani, "Scaling up dynamic time warping for datamining applications," in *Proc. 6th ACM SIGKDD Int Conf. Knowl. Discovery Data Mining*, 2000, pp. 285–289.

[22] Y. He and Y. Li, "Physical activity recognition utilizing the built-in kinematic sensors of a smartphone," *Int. J. Distrib. Sens. Netw.*, vol. 2013, Oct. 2013.

[23] F. Miao, Y. He, J. Liu, Y. Li, and I. Ayoola, "Identifying typical physical activity on smartphone with varying positions and orientations," *Biomed. Eng. Online.*, vol. 14, Apr. 2015.

[24] A. M. Khan, Y.-K. Lee, S. Y. Lee, and T.-S. Kim, "A triaxial accelerometer-based physical-activity recognition via augmented-signal features and a hierarchical recognizer," *IEEE Trans. Inf. Technol. Biomed.*, vol. 14, no. 5, pp. 1166–1172, Sep. 2010.

[25] R. Pan, D. Chua, J S. Pathmasuntharamand, and Y. P. Xu, "An opportunistic relay protocol with dynamic scheduling in wireless body area sensor network," *IEEE Sens. J.*, vol. 15, no. 7, pp. 43743–3750, Jul. 2015.